Immunotherapy Advances, 2025, **5**, ltaf012
https://doi.org/10.1093/immadv/ltaf012
Advance access publication 22 March 2025
Research Article

Intra-tumoural RAMP1+ B cells promote resistance to neoadjuvant anti-PD-1-based therapy in oesophageal squamous cell carcinoma

Hongyu Zhang[1,‡], Yuchen Zhang[1,‡], Pingjing Zhou[1], Yifan Guo[1], Liqun Jiang[2,*], Jie Gu[1,*]

[1]Department of Thoracic Surgery, Zhongshan Hospital, Fudan University, Shanghai, China
[2]Department of Thoracic Surgery, Jingjiang People's Hospital Affiliated to Yangzhou University, Jingjiang, China

[‡]These authors contributed equally to this work.
[*]Corresponding author. Department of Thoracic Surgery, Jingjiang People's Hospital Affiliated to Yangzhou University, Jingjiang, China. E-mail: 15961070011@163.com (L.J.); Department of Thoracic Surgery, Zhongshan Hospital, Fudan University, Shanghai, China. E-mail: gu.jie3@zs-hospital.sh.cn (J.G.)

Abstract

Introduction: The application of neoadjuvant immunotherapy in oesophageal squamous cell carcinoma (ESCC) reactivates anti-tumour immune responses and prolong postoperative survival. However, due to the heterogeneity of tumour microenvironment, limited patients have achieved pathological regression after treatment. The dual roles of B cells were recently highlighted in ESCC. The study aimed to investigate the role of B cell subclusters and the upstream signalling of B cell differentiation in ESCC resistant to immunotherapy.

Methods: Single-cell RNA sequencing was employed for ESCC specimens with distinct responses to neoadjuvant immunotherapy to map the landscape of intra-tumoural B cells.

Results: A novel subset of neuropeptide receptor, receptor activity-modifying protein 1 (RAMP1) positive B cells was revealed to accumulate in ESCC that is resistant to neoadjuvant immunotherapy. Stimulated by nociceptor neurons secreting calcitonin gene-related peptide (CGRP), RAMP1(+) B cells exhibit an immunosuppressive phenotype. The elevated secretion of immune-regulating cytokines by RAMP1(+) B cells blunts the cytotoxicity of Cluster of Differentiation (CD)8(+) T cell and leads to tumour immune evasion. A combination of RAMP1 blocker and anti-Programmed cell death protein (PD)-1 therapies synergistically reinvigorated anti-tumour immunity, reducing tumour progression *in vitro*.

Conclusion: The study suggests that RAMP1(+) B cells play a critical role in mediating resistance to neoadjuvant immunotherapy in ESCC. Targeting the CGRP-RAMP axis remodels B cells and enhance the efficacy of current immunotherapies, providing new strategies for overcoming treatment resistance.

Received: December 29, 2024; Accepted: March 17, 2025

Graphical Abstract

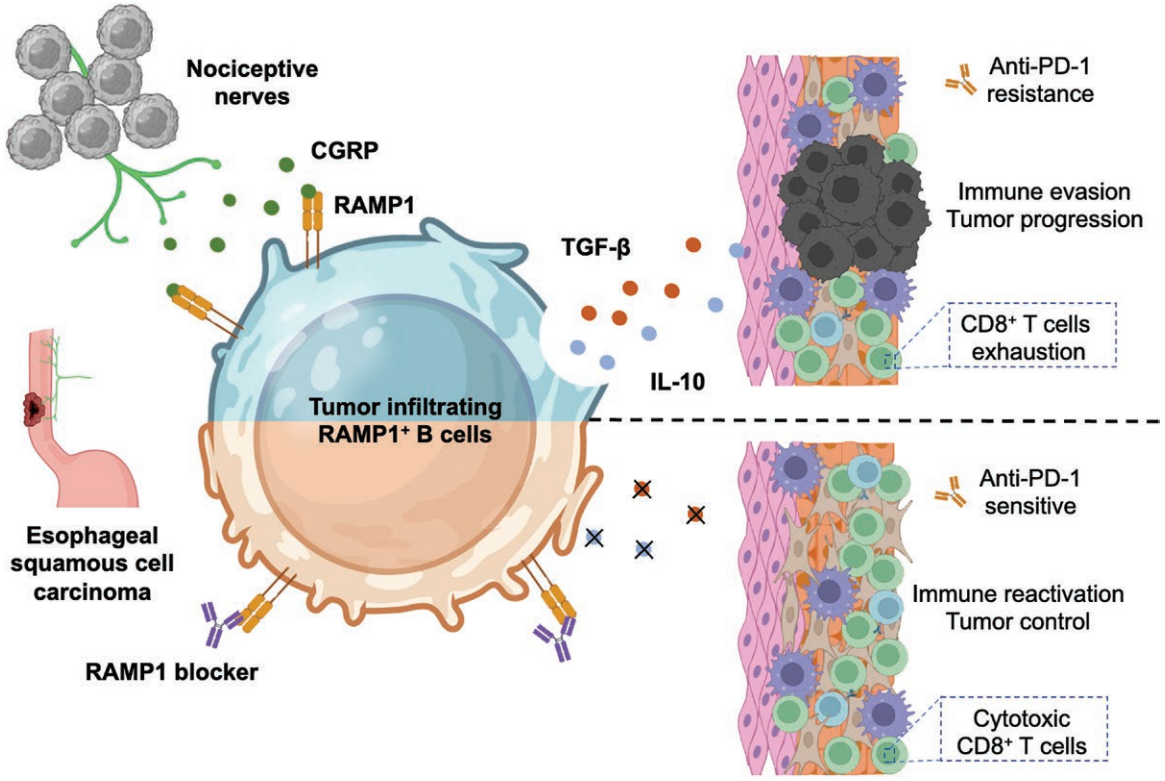

Keywords: B cell; neuroimmunology; immunotherapy; regulation; suppression

Introduction

Immune checkpoint inhibitors (ICIs) have revolutionized cancer treatment, with anti-PD-1 monoclonal antibodies emerging as first-line therapies for advanced or metastatic oesophageal squamous cell carcinoma (ESCC) [1]. Clinical trials have demonstrated that neoadjuvant treatments incorporating ICIs can reinvigorate anti-tumour immunity, reduce tumour burden, and restore the opportunity for curative surgery [2, 3].

However, responses to neoadjuvant immunotherapy remain highly heterogeneous, with about half of ESCC patients achieving pathological downstaging and survival benefits [4]. Recent insights into the tumour immune microenvironment (TIME) highlight B cell infiltration and tertiary lymphoid structures as key regulators of anti-tumour immunity, functioning through antigen presentation, co-stimulatory signals, and antibody secretion [5, 6]. Nevertheless, regulatory B cells have been reported to promote tumour growth in gastrointestinal cancers by secreting immunosuppressive cytokines such as Interleukin (IL)-10 and Transforming growth factor beta (TGF-β) [7, 8]. This dual role of B cells in tumour progression underscores the importance of elucidating their function within the ESCC microenvironment.

The oesophagus, richly innervated by autonomic and sensory nerves, experiences nociceptive activation in conditions like reflux disease and ischaemia [9, 10]. Nociceptive receptors have been identified as critical immune modulators, capable of alleviating or exacerbating inflammation [11]. Calcitonin gene-related peptide (CGRP), released upon Transient receptor potential vanilloid 1 (TRPV1)-positive nociceptive nerve activation, has been linked to heightened expression of immune checkpoint receptors on CD8⁺ T cells [12, 13]. The receptor activity-modifying protein 1 (RAMP1), a major CGRP target, facilitates the localization of the calcitonin-like receptor on the cell membrane and activates downstream signalling pathways [14]. Emerging evidence suggests that CGRP-secreting sensory neurons regulate immune cell aggregation, promote apoptosis, and enhance macrophage efferocytosis via RAMP1 [15]. Whether such neural activity modulates B cell functions and contributes to therapy resistance warrants further investigation.

Here, we revealed that RAMP1⁺ B cells were significantly elevated in poor responders to immune therapy, secreting high levels of anti-inflammatory cytokines. Since the CGRP-RAMP1 axis have been identified with immunomodulatory potential, we further investigate RAMP1⁺ B cells as key mediators of immunosuppression in ESCC. Our findings highlight that targeting the CGRP-RAMP1 axis holds clinical potential by remodelling the immunosuppressive phenotype of RAMP1⁺ B cells, thereby enhancing CD8⁺ T cell effector functions and improving the efficacy of anti-PD-1 treatment in ESCC.

Materials and methods

Patients

This study enrolled patients with ESCC treated with standard neoadjuvant immunotherapy and chemotherapy at Zhongshan Hospital, Fudan University, from 2021 to 2024. Post-treatment ESCC samples from 10 patients treated with anti-PD1 plus paclitaxel and platin-based chemotherapy were collected for single-cell RNA sequencing. Among them, five patients received Pembrolizumab, three received Nivolumab, and two

received Camrelizumab. Additionally, 24 pre-treatment tissue samples were preserved in formalin-fixed paraffin-embedded (FFPE) blocks, sectioned, and prepared for multiplex immunofluorescence analysis. Six post-treatment ESCC samples and five untreated ESCC samples collected in 2024 were used for flow cytometry analysis. Therapeutic responses were evaluated using the Mandard tumour regression grade, with grades 1–2 classified as responders and grades 3–5 as non-responders. The study was approved by the Ethics Committee of Zhongshan Hospital, Fudan University (B2021-129).

Single-cell RNA sequencing data analysis

Transcriptome data for B cells were obtained from 24 samples across two ESCC scRNA-seq datasets (HRA006065 and GSE145370). The HRA006065 cohort included patients who received neoadjuvant immune-chemotherapy, while the GSE145370 cohort comprised surgical ESCC samples and paired peri-tumour samples.

Matrix files were imported into R (version 4.2.1) and analysed using Seurat (version 4.3.0). Cells with >200 detected genes and total transcript counts between 200 and 6000 were selected for analysis. Cells with >30% mitochondrial gene transcripts were excluded due to potential apoptosis. Integration and batch-effect correction were performed using the Harmony algorithm. Within 134 241 $CD45^+$ cells after quality control, major cell clusters were identified with CellTypist (version 1.6.2), and 18 047 B cells, defined by high expression of CD79A, CD79B, CD19, MS4A1, MZB1, and JCHAIN, were extracted. B cells underwent normalization, variable feature selection, data scaling, and Uniform Manifold Approximation and Projection (UMAP) dimensionality reduction. Sub-clustering was performed with Clustree (version 0.5.0) at a resolution of 1.0. Marker genes were identified using the FindAllMarkers function.

Bulk RNA sequencing data source and processing

Patient characteristics from the The Cancer Genome Atlas (TCGA)-ESCC cohort were retrieved via cBioPortal. The immune checkpoint blockade (ICB) cohort included 366 patients with solid tumours treated with atezolizumab (GO29293 cohort [16]). A $RAMP1^+$ B cell gene signature was derived from the top 20 expressed genes of the RAMP1_B subcluster in scRNA-seq data. The Gene Set Variation Analysis (GSVA) package (version 1.48) calculated single sample Gene Set Enrichment Analysis (ssGSEA) scores for each signature across TCGA-ESCC and ICB cohorts.

Multiplex immunohistochemistry

FFPE tumour sections were baked at 60°C for 5 h, deparaffinized in xylene (three cycles), and rehydrated in graded alcohol. Antigen retrieval was performed by heating sections in sodium citrate buffer (0.01 M, pH 6) for 20 min. Slides were incubated with 10% normal goat serum at 37°C for 20 min to block non-specific binding, followed by primary antibody incubation for 2 h at 37°C. Co-staining was performed using a multi-colour fluorescence kit (Recordbio Biological Technology, Shanghai, China) based on tyramide signal amplification, following the manufacturer's instructions. Slides were mounted with 4',6-diamidino-2-phenylindole (DAPI)-containing antifade solution.

Isolation of lymphocytes and co-culture

Peripheral blood mononuclear cells (PBMCs) were isolated using a lymphocyte separation medium (KLSH1408, Dakewe Biotech). Briefly, 10 ml of whole blood was layered onto 5 ml of separation medium in a 15-ml tube. After centrifugation at 800g for 20 min, PBMCs were collected from the interface, washed three times with phosphate buffered saline (PBS), and separated into B and T cells using the EasySep™ Human B Cell and $CD8^+$ T Cell Isolation Kits (Stemcell Technologies, #17954 and #19663, respectively), following the manufacturer's protocols.

Tumour tissue was weighed, washed with PBS, and centrifuged through a 20-mm nylon mesh at 400g for 15 min. Tumour interstitial fluid (TIF) was collected and used for B cell culture. B cells (5×10^5/well) were seeded in Roswell Park Memorial Institute (RPMI)-1640 medium with 10% FBS, 10 μg/ml lipopolysaccharide, and matched TIF, and treated with $CGRP_{8\text{-}37}$ (2 μg/ml, TOCRIS Bioscience, #1181) as a CGRP antagonist. Cultures were incubated at 37°C with 5% CO2 for 24 h.

For co-culture of B cells and T cells, $CD45^+CD19^+RAMP1^+$ B cells and $CD45^+CD19^+RAMP1^-$ B cells were sorted from ESCC on the BD FACsAria flow cytometer. Sorted B cells (2×10^4 cells/well) and $CD8^+$ T cells (2×10^5 cells/well) from the PBMC of same patient were plated in 48-well U-bottom plates and co-cultured for 48 h with anti-CD3 (2 μg/ml), anti-CD28 (10 μg/ml), interleukin-2 (0.2 μg/ml), anti-IgM (2 μg/ml), and lipopolysaccharide (10 μg/ml). Flow cytometry was used to evaluate lymphocyte function.

Flow cytometry

Cells were suspended in 100 μl of PBS with 1% Bovine Serum Albumin (BSA) and 0.05% NaN3, and incubated with fluorochrome-conjugated antibodies for 30 min at 4°C. After washing, intracellular staining was performed using the Foxp3 Transcription Factor Staining Buffer Set (Thermo Fisher, 00-5123-43). For intracellular cytokine analysis, cells were stimulated *in vitro* with a cell stimulation cocktail (Thermo Fisher, 00-4975-93) for 5 h, followed by fixation, permeabilization, and staining with monoclonal antibodies. Fluorescence data were acquired on a BD FACSCelesta Multicolor Flow Cytometer and analysed using FlowJo software. The antibodies used were listed in Supplementary Table 1.

In vitro intervention assay

Tumour tissues from five patients with ESCC were collected to perform *in vitro* intervention assays. Single-cell suspensions of tumour cells were cultured with the RAMP1 blocker $CGRP_{8\text{-}37}$ (2 μg/ml), PD-1 antibody (5 μg/ml, A2002, Selleck), or Immunoglobulin G (IgG) 4B κ isotype control antibodies (10 μg/ml, A1101, Biovision) in RPMI-1640 medium supplemented with 10% Fetal Bovine Serum (FBS). After 12 h culture, the suspensions were analysed via flow cytometry to assess cellular functions.

Statistical analysis

Continuous variables were analysed using the Student's t-test ($n < 30$) or Mann–Whitney U test ($n > 30$). Box plots displayed medians (centre line), 25th and 75th percentiles (box limits), and standard deviations (error bars). Kaplan–Meier curves assessed progression-free survival, with group comparisons using the log-rank test. Multivariate logistic regression identified variables and potential confounders. Statistical tests are detailed in figure legends. Medians were used as cut-offs to categorize samples by high or low values. Analyses were performed in R (version 3.4) and IBM SPSS Statistics (version 26.0), with a two-sided P-value <.05 considered significant.

Results

Single-cell atlas reveals the infiltration of RAMP1^{+} B cells in ESCC resistant to immunotherapy

High-throughput single-cell RNA sequencing was performed to investigate the B cell landscape within 24 surgical samples from 17 patients with pathologically confirmed ESCC (Fig. 1A), including peri-tumoural oesophageal tissue, untreated ESCC, neoadjuvant immunotherapy-responsive ESCC, and resistant ESCC (Fig. 1B). After dimensionality reduction, clustering of B cells by canonical B cell markers (Fig. 1C) identified eight subpopulations, including FOXP1_Bn, YBX3_Bn, ITGB1_Bm, IFIT3_B, Bpre_gc, Bgc, plasma cells, and a previously uncharacterized subset of RAMP1_B cells. The feature of marker genes for each B cell subsets was shown in Fig. 1D. Notably, comparative analysis revealed a significant elevation of RAMP1_B cells in the treatment-resistant group (26.1%) compared to the responsive group (4.4%) (Fig. 1E). RAMP1_B cells exhibited high expression of activated B cell markers, implying that they had undergone affinity maturation in germinal centres and may orchestrate immune responses in the TIME of treatment-resistant ESCC.

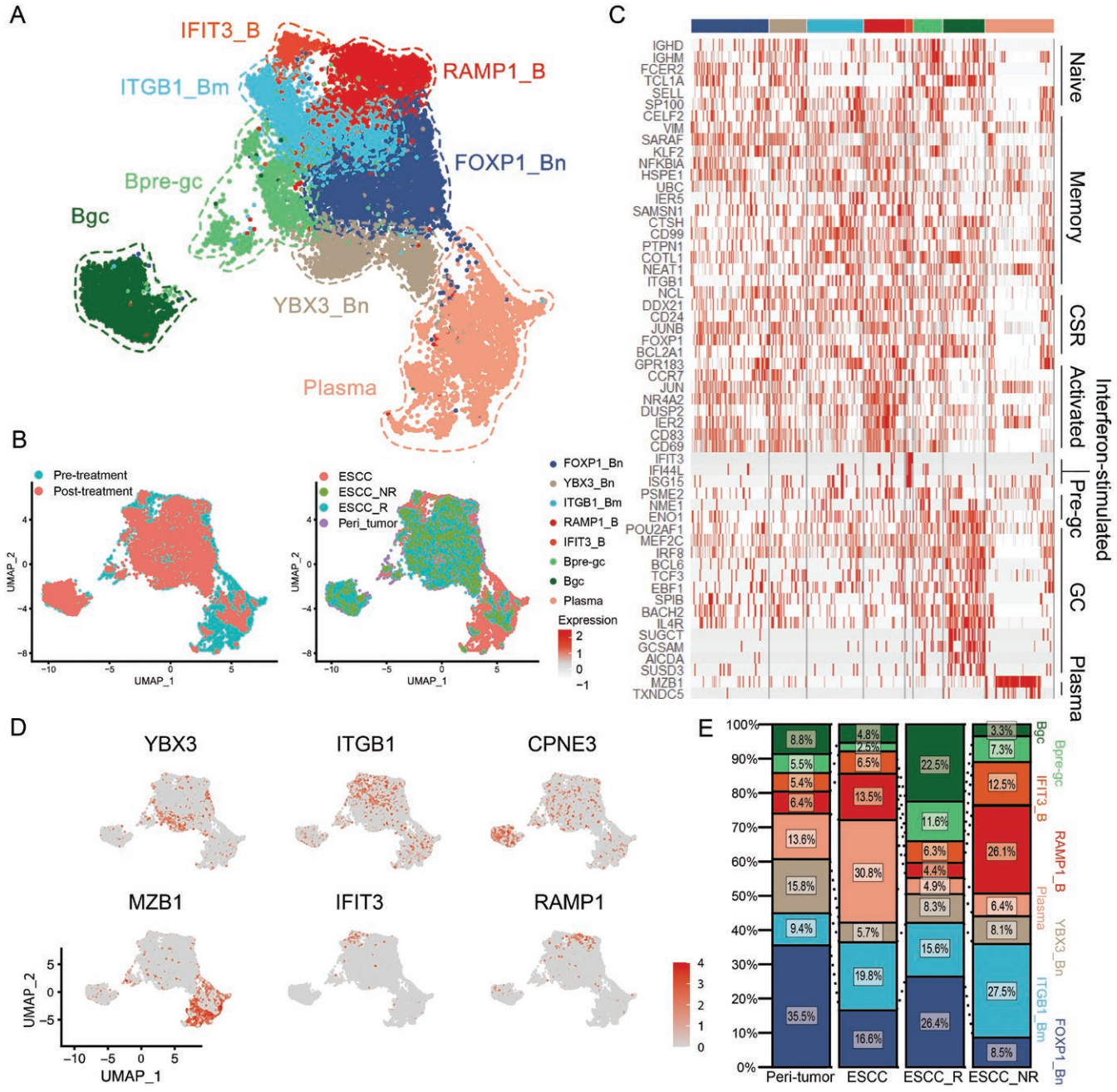

Figure 1. Single-cell landscape for B cells infiltrated in ESCC before and after immunotherapy. (A–B) UMAP visualization of all B cells enrolled, colored by cell types (A), treatment, and sample types (B). (C) Heatmap of characteristic genes in clustered B cell subsets. (D) Feature plot of characteristic genes for B cell subsets. (E) Bar chart of the proportions of B cell subsets in different ESCC sample types.

RAMP1+ B cells are associated with resistance to neoadjuvant immunotherapy and poor prognosis

To further investigate the prognostic relevance of RAMP1⁺ B cell and correlating nociceptive sensory neurons and neuropeptide, we applied immunofluorescence analysis on pre-neoadjuvant immunotherapy ESCC samples from 24 patients (Fig. 2A and B). The infiltration of pre-treatment RAMP1⁺ CD19⁺ B cells was elevated in non-responding patients. Also, TRPV1⁺ nociceptive neurons, which secrete the neuropeptide CGRP, were significantly more abundant in resistant ESCC tissues (Fig. 2C), suggesting that the CGRP-RAMP1 signalling axis may contribute to immunotherapy resistance. Further, pre-treatment RAMP1⁺ B cell infiltration levels were identified as an independent predictive marker for neoadjuvant immunotherapy response in the multivariable logistic regression analysis (Fig. 2D). The predictive potency of RAMP1⁺ B cell infiltration was also found to be independent of total B cell infiltration (Supplementary Fig. 1A). Using upregulated genes in RAMP1_B cell clusters, a RAMP1⁺ B cell gene signature was generated and was found to increase among the B cells from non-responders (Fig. 2E).

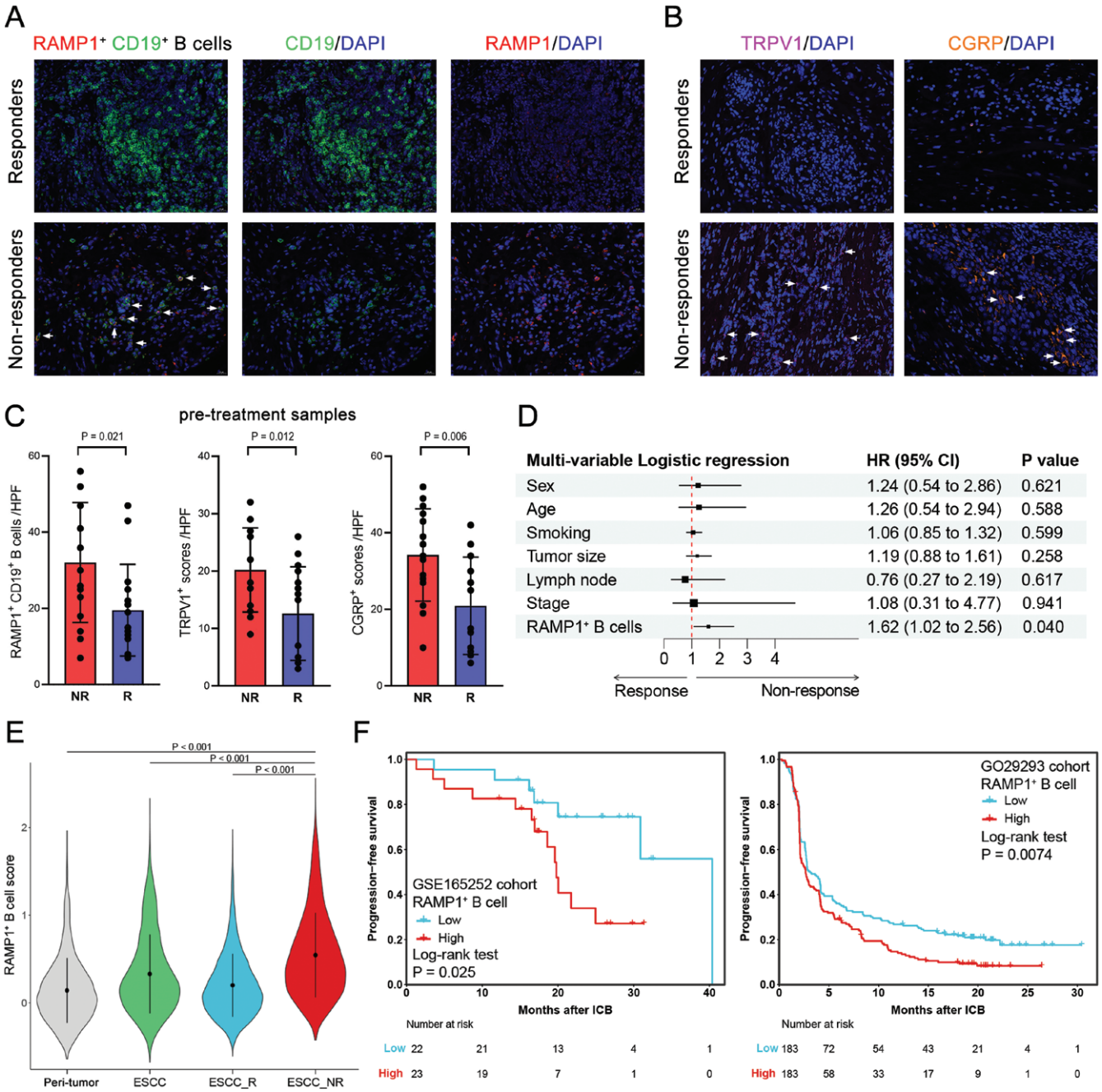

Figure 2. RAMP1⁺ B cells are associated with resistance to neoadjuvant immunotherapy in ESCC. (A) Representative immunofluorescence staining of ESCC for CD19 and RAMP1. (B) Representative immunofluorescence staining of ESCC for TRPV and CGRP. (C) Comparison of RAMP1⁺ CD19⁺ cells, TPRV1⁺ scores, and CGRP⁺ scores between responding and non-responding ESCC before treatment (Student's t-test). (D) Forest plot representing the odd ratios with error bars corresponding to 95% CI bounds determined by the multivariable Logistic regression model. (E) Violin plot showing comparison of RAMP1⁺ B cell signature between B cells from different sample types (Mann–Whitney U test). (F) Progression-free survival curves generated for RAMP1⁺ B cell signatures in patients treated with immunotherapy (Log-rank test).

In TCGA-ESCC cohort, the RAMP1⁺ B cell score showed no discrepancy in tumours with different T stages, N stages, and grades (Supplementary Fig. 1B). External oesophageal cancer immunotherapy datasets and pan-cancer cohorts further revealed a strong association between RAMP1⁺ B cells and adverse long-term prognosis after immunotherapy (Fig. 2F).

RAMP1+ B cells exhibit regulatory B cell functions

The analyses above implicated that RAMP1⁺ B cells may play a vital role in mitigating immune responses. Further functional profiling of RAMP1⁺ B cells by single-cell RNA sequencing data revealed upregulation of immune-regulatory molecules (TNFRSF9, FCRL4, and ITGAX) [17] and B cell activation markers (CD69 and IER2), compared to RAMP1⁻ B cells (Fig. 3A). Moreover, GSVA scoring of B cells indicated that cell cycle and TGF beta pathways were enriched in RAMP1⁺ B cells (Fig. 3B). At the protein level, flow cytometric analysis validated the presence of RAMP1⁺ B cells in treatment-resistant ESCC (Fig. 3C). Also, upregulation of RAMP1⁺ B cells was found in ESCC compared to matched peri-tumour samples (Fig. 3D), suggesting that they were potentially involved in tumour progression. Also, immunoregulatory cytokines TGF-β and IL-10 was dominantly secreted by RAMP1⁺ B cells (Fig. 3E and F), consistent with the phenotype of regulatory B cells.

To investigate the microenvironmental factors contributing to RAMP1⁺ B cell induction, TIF was prepared from fresh ESCC tissue samples and used to stimulate isolated B cells. TIF stimulation significantly enhanced the secretion of TGF-β and IL-10 by B cells. Notably, the addition of a CGRP antagonist to the TIF-stimulated culture system markedly reduced the levels of immunoregulatory molecules (Fig. 3G). These results indicate that the CGRP-RAMP1 axis plays a pivotal role in inducing the immunosuppressive phenotype of B cells in the ESCC microenvironment.

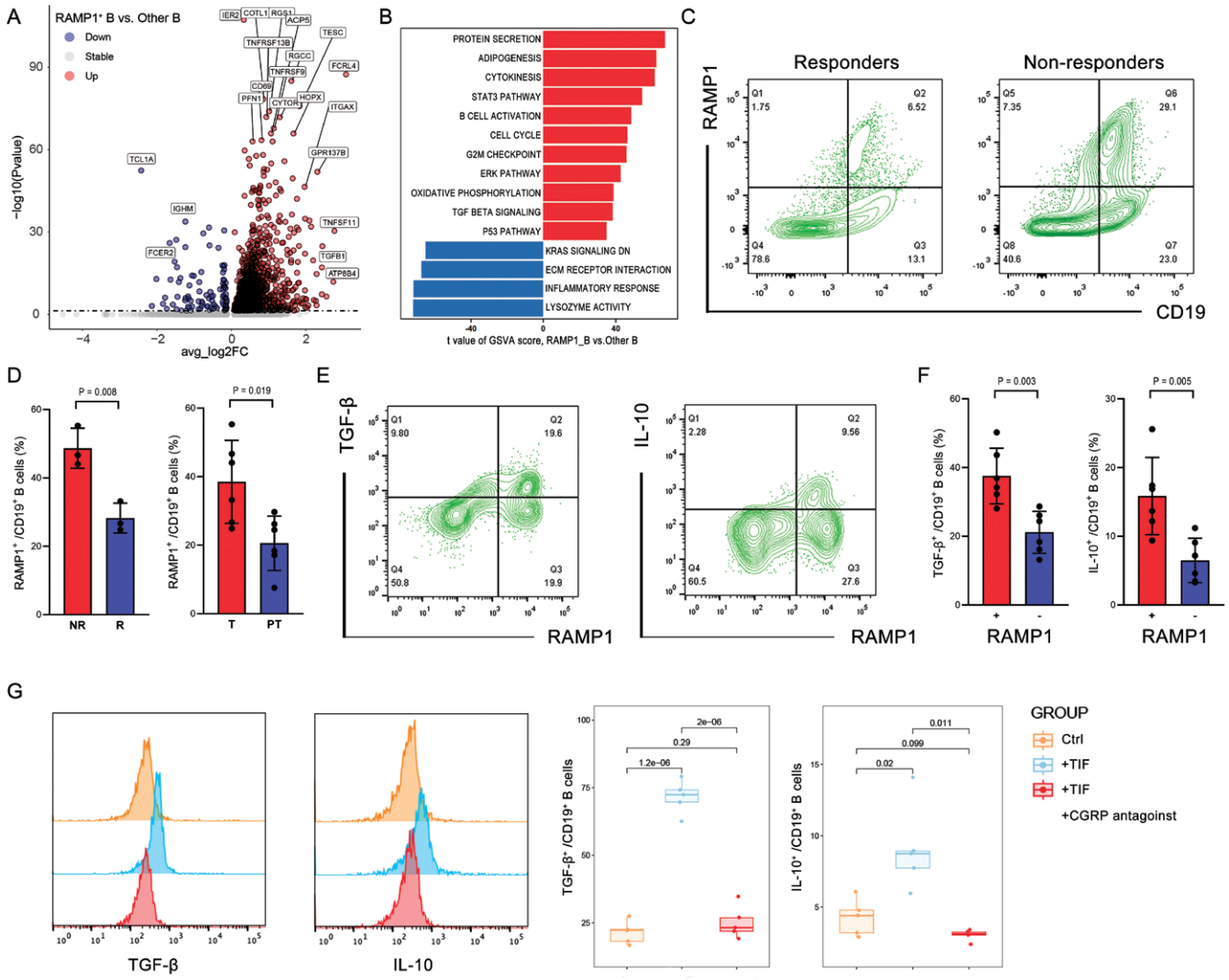

Figure 3. CGRP mediates the immunosuppressing phenotypes of RAMP1⁺ B cells. (A) Volcano plot showing differentially expressed genes between RAMP1⁺ B cells and RAMP1⁻ B cells. (B) Differential pathway enriched in RAMP1⁺ B cells and RAMP1⁻ B cells by GSVA. Two-sided unpaired limma-moderated t-test. (C) Representative flow cytometric plots of RAMP1⁺ B cells in responding and non-responding ESCC. (D) Comparison of the percentage of RAMP1⁺ B cells in ESCC with different responds to immunotherapy (left) and different sample types (right) (Student's t-test). (E) Representative flow cytometric plots depicting the phenotype of RAMP1⁺ B cells with TGF-β and IL-10. (F) Comparison of the percentage of TGF-β and IL-10 expression between RAMP1⁺ B cells and RAMP1⁻ B cells (Student's t-test). (G) Representative histograms of TGF-β and IL-10 expression in B cells stimulated by tumour interstitial fluid in the absence or presence of the CGRP antagonist and corresponding statistical analysis (Student's t-test).

RAMP1+ B cells impair CD8+T cell effector functions in ESCC

Subsequently, the influence of RAMP1$^+$ B cells on immune contexture in ESCC was addressed. We performed CIBERSORT to calculate the relative proportion of 18 immune cell types within the TCGA-ESCC database. High RAMP1$^+$ B cell signature was associated with low level of CD8$^+$ T cells, M1 macrophages, and activated memory CD4$^+$ T cells (Fig. 4A). Co-culture experiments were further implemented to investigate the role of RAMP1$^+$ B cells in suppressing CD8$^+$ T cell effector functions (Fig. 4B). Of note, RAMP1$^+$ B cells induced functional exhaustion in CD8$^+$ T cells, reducing the expression of anti-tumour molecules Interferon (IFN)-γ and CD107a while upregulating immune checkpoint markers PD-1 and Lymphocyte-activation gene (LAG)-3, rather than RAMP1$^-$ B cells (Fig. 4C and D). Collectively, these findings suggest that RAMP1$^+$ B cells act as an immunosuppressive B cell subset with critical properties in regulating CD8$^+$ T cell functions in ESCC.

RAMP1 blockade synergizes with anti-PD-1 therapy in reinvigorating anti-tumour immunity

As RAMP1$^+$ B cells exert immune-regulating effects in patients resistant to immunotherapy, we explore the treatment of RAMP1 blocker for these patients using an *in vitro* intervention model with fresh ESCC tissues (Fig. 5A). Four groups of intervention were designated, namely, control group, RAMP1 blocker group, Anti-PD-1 group, and combined treatment group. After treated by RAMP1 blocker and combined regimen, B cells exhibit less secretion of TGF-β and IL-10 (Fig. 5B). Meanwhile, RAMP1 blocker treatment showed profound enhancements in the infiltration and proliferation of CD8$^+$ T cells (Fig. 5C and D). Degranulation and cytotoxicity functions of CD8$^+$ T cells were also augmented by RAMP1 blocker. Remarkably, the combination regimen of RAMP1 blocker and anti-PD-1 further boosted the anti-tumour function of CD8$^+$ T cells than applying the antibody alone (Fig. 5E). In addition, apoptosis of tumour cells was enhanced by RAMP1 blocker, while proliferation of tumour cells was decreased by RAMP1 blocker and further mitigated by combined therapy (Fig. 5F). Overall, these findings indicated that the combined therapy of RAMP1 blocker and anti-PD-1 results in enhanced CD8$^+$ T cells effector function, which may potentially benefit patients resistant to anti-PD-1-based immunotherapy.

Discussion

Our study delineates a comprehensive single-cell blueprint of B cells infiltrated in ESCC and sheds light on the pivotal role of RAMP1$^+$ B cells in mediating resistance to neoadjuvant immunotherapy. We demonstrate that RAMP1$^+$ B cells represent an immunosuppressive subset linked to adverse clinical outcomes, mediated by the CGRP-RAMP1 signalling axis, offering new insights into the interplay between the TIME and neural-immune signalling pathways.

Previous studies have stated the duality of B cell functions in ESCC, wherein distinct subsets can either promote or inhibit anti-tumour immunity [8]. RAMP1$^+$ B cells were identified as an immunosuppressive subset, exhibiting unique features, including heightened expression of immune-regulatory molecules (IL-10 and TGF-β) and activation markers (CD69 and IER2), which further declared the induction of regulatory

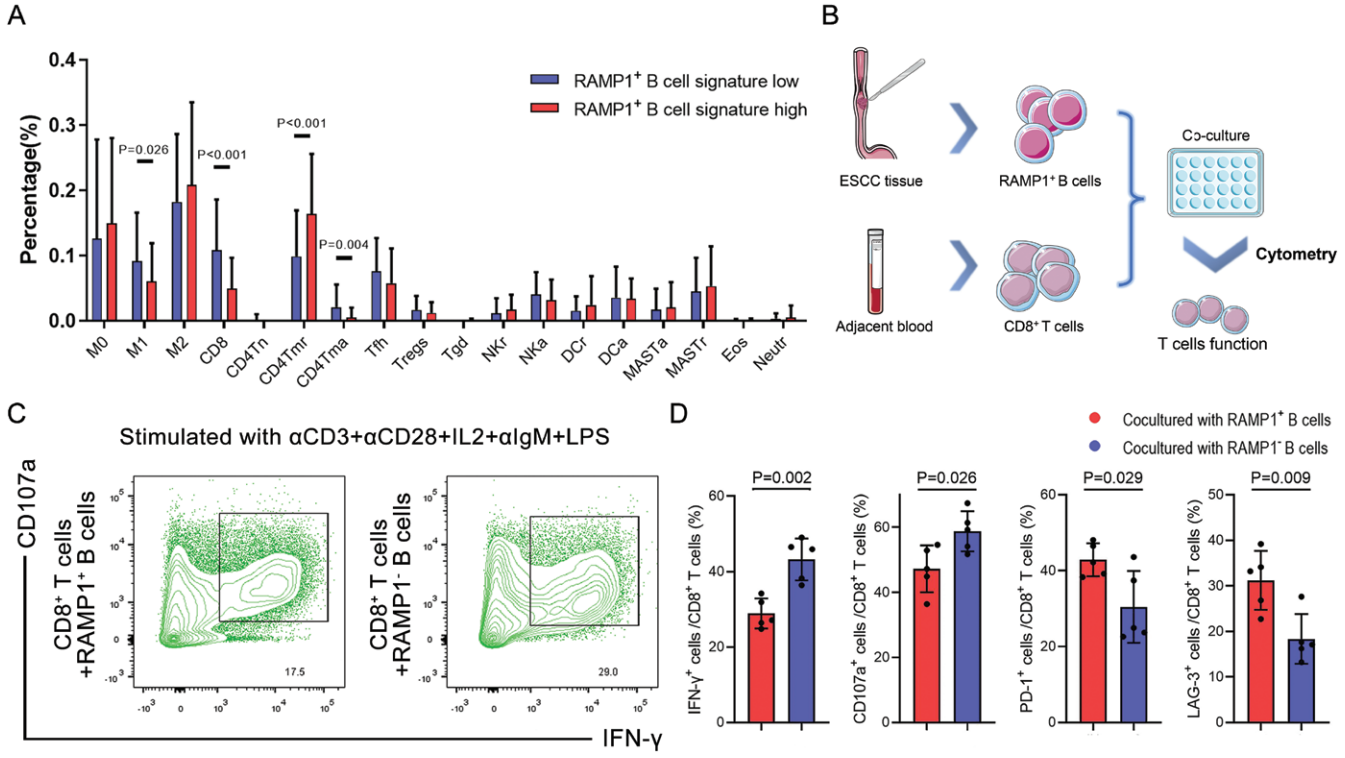

Figure 4. RAMP1$^+$ B cells infiltration impairs CD8$^+$T cell function in ESCC. (A) Comparison of immune cell infiltrations between ESCC with different RAMP1$^+$ B cell signature levels (Mann–Whitney U test). (B) Co-culture of RAMP1$^{+/-}$ B cells from ESCC and CD8$^+$T cells from adjacent blood to followed by examination of CD8$^+$T cell functions. (C) Representative flow cytometric plots of T cell degranulation and cytotoxicity after co-culture of CD8$^+$T cells and RAMP1$^{+/-}$ B cells. (D) Statistical analysis of T cell degranulation, cytotoxicity, and exhaustion after co-culture (Student's t-test).

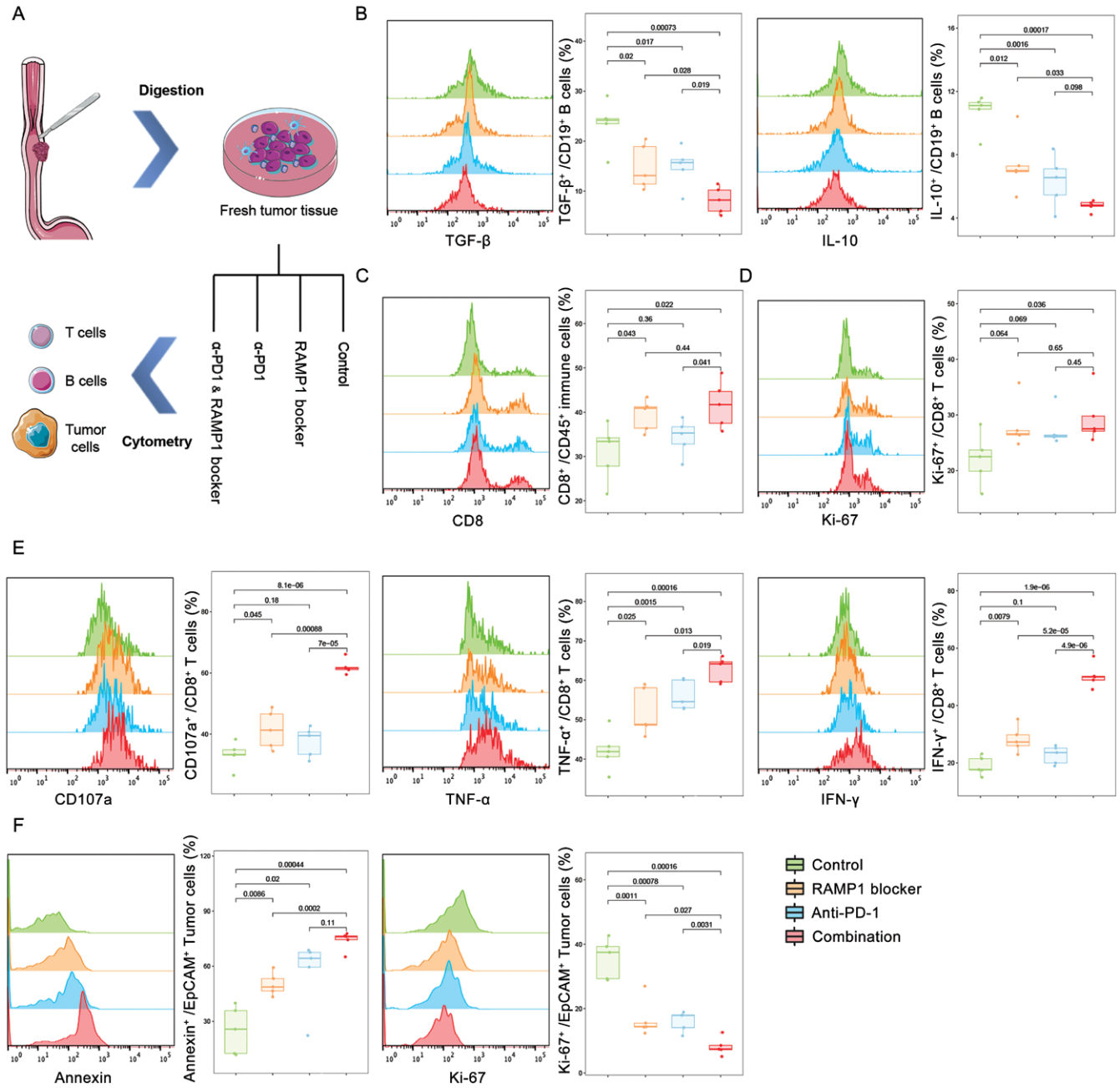

Figure 5. RAMP1 blockade synergizes with anti-PD-1 therapy in reinvigorating anti-tumour immunity. (A) An *in vitro* intervention model was established using fresh ESCC tissues to assess the ability of RAMP1 blocker and anti-PD1 antibody to reactivate immune responses. (B) The secretion of immunoregulating molecules by B cells after the blockade of RAMP1 and PD-1 (Student's t-test). (C–D) The infiltration and proliferation of $CD8^+$ T cells after the blockade of RAMP1 and PD-1 (Student's t-test). (E) The degranulation and cytotoxicity of $CD8^+$ T cells after the blockade of RAMP1 and PD-1 (Student's t-test). (F) The apoptosis and proliferation of tumour cells after the blockade of RAMP1 and PD-1 (Student's t-test).

B cells requires B cell activating signals [18, 19]. Moreover, our findings indicate that $RAMP1^+$ B cells orchestrate an immunosuppressive microenvironment by reducing the cytotoxic potential of $CD8^+$ T cells. This interaction underscores the critical role of $RAMP1^+$ B cell subsets in shaping immune contexture and tumour progression.

The identification of $RAMP1^+$ B cells bridges the gap between neural signalling and immune modulation, positioning sensory neurons as critical regulators of TIME. Previous studies have revealed innervation of sensory fibres in lymph nodes and tumours, where they regulate immune responses through neuropeptide release [12, 20]. Here, we identified the presence of $TRPV1^+$ sensory innervation in ESCCs. The plausible mechanisms through which sensory neurons detect the progression of tumours have been established [21], and we illustrated that by secreting neuropeptide CGRP, nociceptor neurons regulate the function of B cells, leading to an immunosuppressive phenotype. By demonstrating the CGRP-RAMP1 axis as a mediator of B cell polarization, this research highlights a previously underexplored mechanism of immune dysfunction, providing a framework for future studies on neuro-immune crosstalk in cancer.

The significant enrichment of $RAMP1^+$ B cells in treatment-resistant ESCC also underscores their potential as predictive

biomarkers and therapeutic targets for immunotherapy. Multivariate analysis confirmed that pre-treatment RAMP1$^+$ B cell levels are independently associated with poor outcomes, consistent with observations in external cohorts. Strategies aimed at reducing the influence of RAMP1$^+$ B cells, such as RAMP1 antagonism, were proved to reinvigorate CD8$^+$ T cell function, promoting effective anti-tumour responses. Targeting the CGRP-RAMP1 pathway may thus disrupt this immunosuppressive crosstalk, offering a novel approach to counteract immune resistance. Moreover, the observed synergy between RAMP1 blockers and anti-PD-1 therapies represents a significant advancement in overcoming immunotherapy resistance. By simultaneously targeting B cell-mediated suppression and reactivating CD8$^+$ T cells, this dual approach could address the limitations in current immunotherapeutic regimens.

While our study provides evidence of the immunosuppressive role of RAMP1$^+$ B cells, several limitations warrant further exploration. The observational nature of our analyses and the limited sample size may constrain the generalizability of our findings. Additionally, the molecular mechanisms underlying CGRP-mediated RAMP1$^+$ B cell activation remain incompletely understood. Exploring the molecular pathways downstream of CGRP-RAMP1 signalling in B cells could uncover additional targets for therapeutic intervention. Future studies will focus on elucidating the broader implications of intervention on sensory neurone-immune interactions in solid tumours.

Overall, this study not only elucidates the role of RAMP1$^+$ B cells as mediators of immunosuppression but also underscores the therapeutic potential of targeting the CGRP-RAMP1 axis in ESCC. The influence of RAMP1$^+$ B cells on CD8$^+$ T cell dysfunction and immune evasion positions them as promising targets for reprogramming intra-tumoural B cells and overcoming resistance to immunotherapy. The combination therapies of RAMP1 blocker and anti-PD-1 exhibited the efficacy to reactivate CD8$^+$ T cells and the potential to transform clinical outcomes for patients with ESCC. By integrating neural and immune perspectives, our findings contribute to the growing evidence supporting the importance of targeting B cell subsets to optimize current immunotherapy.

Supplementary material

Supplementary data are available at Immunotherapy Advances online.

Acknowledgements

The Editor-in-Chief, Tim Elliott, and handling editor, Yiwei Chu, would like to thank the two anonymous reviewers for their contribution to the publication of this article.

Author contributions

Hongyu Zhang (Data curation, Formal analysis, Investigation, Resources, Software, Visualization, Writing—original draft), Yuchen Zhang (Formal analysis, Resources, Validation), Pingjing Zhou (Formal analysis, Software, Validation), Yifan Guo (Methodology, Resources, Software), Liqun Jiang (Funding acquisition, Methodology, Supervision), and Jie Gu (Conceptualization, Funding acquisition, Project administration, Supervision, Writing—review & editing)

Conflict of interest: None declared.

Ethical approval

The study was approved by the Ethics Committee of Zhongshan Hospital, Fudan University (B2021-129).

Funding

This study was provided by the National Science Foundation of China (82403959 and 82373371), China Postdoctoral Science Foundation (2024M760550), and Outstanding Resident Clinical Postdoctoral Program of Zhongshan Hospital Affiliated to Fudan University.

Data availability

This study did not generate new sequence data. Deidentified individual participant data of this study are available from the corresponding author upon request.

References

1. Xu J, Kato K, Raymond E et al. Tislelizumab plus chemotherapy versus placebo plus chemotherapy as first-line treatment for advanced or metastatic oesophageal squamous cell carcinoma (RATIONALE-306): a global, randomised, placebo-controlled, phase 3 study. *Lancet Oncol* 2023; 24:483–95. https://doi.org/10.1016/S1470-2045(23)00108-0
2. Yang Y, Zhu L, Cheng Y et al. Three-arm phase II trial comparing camrelizumab plus chemotherapy versus camrelizumab plus chemoradiation versus chemoradiation as preoperative treatment for locally advanced esophageal squamous cell carcinoma (NICE-2 Study). *BMC Cancer* 2022; 22:506. https://doi.org/10.1186/s12885-022-09573-6
3. Li C, Zhao S, Zheng Y et al. Preoperative pembrolizumab combined with chemoradiotherapy for oesophageal squamous cell carcinoma (PALACE-1). *Eur J Cancer* 2021; 144:232–41. https://doi.org/10.1016/j.ejca.2020.11.039
4. Li Q, Liu T, Ding Z. Neoadjuvant immunotherapy for resectable esophageal cancer: a review. *Front Immunol* 2022; 13:1051841. https://doi.org/10.3389/fimmu.2022.1051841
5. Cabrita R, Lauss M, Sanna A et al. Tertiary lymphoid structures improve immunotherapy and survival in melanoma. *Nature* 2020; 577:561–5. https://doi.org/10.1038/s41586-019-1914-8
6. Petitprez F, de Reyniès A, Keung EZ et al. B cells are associated with survival and immunotherapy response in sarcoma. *Nature* 2020; 577:556–60. https://doi.org/10.1038/s41586-019-1906-8
7. Wang Z, Lu Z, Lin S et al. Leucine-tRNA-synthase-2-expressing B cells contribute to colorectal cancer immunoevasion. *Immunity* 2022; 55:1067–81.e8. https://doi.org/10.1016/j.immuni.2022.04.017
8. Zhang H, Wen H, Zhu Q et al. Genomic profiling and associated B cell lineages delineate the efficacy of neoadjuvant anti-PD-1-based therapy in oesophageal squamous cell carcinoma. *EBioMedicine* 2024; 100:104971. https://doi.org/10.1016/j.ebiom.2024.104971
9. Orlando RC. Esophageal perception and noncardiac chest pain. *Gastroenterol Clin North Am* 2004; 33:25–33. https://doi.org/10.1016/S0889-8553(03)00133-X
10. Winkler F, Venkatesh HS, Amit M et al. Cancer neuroscience: state of the field, emerging directions. *Cell* 2023; 186:1689–707. https://doi.org/10.1016/j.cell.2023.02.002
11. Baral P, Udit S, Chiu IM. Pain and immunity: implications for host defence. *Nat Rev Immunol* 2019; 19:433–47. https://doi.org/10.1038/s41577-019-0147-2
12. Balood M, Ahmadi M, Eichwald T et al. Nociceptor neurons affect cancer immunosurveillance. *Nature* 2022; 611:405–12. https://doi.org/10.1038/s41586-022-05374-w

13. Russell FA, King R, Smillie SJ et al. Calcitonin gene-related peptide: physiology and pathophysiology. *Physiol Rev* 2014; 94:1099–142. https://doi.org/10.1152/physrev.00034.2013
14. Yang D, Jacobson A, Meerschaert KA et al. Nociceptor neurons direct goblet cells via a CGRP-RAMP1 axis to drive mucus production and gut barrier protection. *Cell* 2022; 185:4190–205.e25. https://doi.org/10.1016/j.cell.2022.09.024
15. Lu YZ, Nayer B, Singh SK et al. CGRP sensory neurons promote tissue healing via neutrophils and macrophages. *Nature* 2024; 628:604–11. https://doi.org/10.1038/s41586-024-07237-y
16. Mariathasan S, Turley SJ, Nickles D et al. TGFβ attenuates tumour response to PD-L1 blockade by contributing to exclusion of T cells. *Nature* 2018; 554:544–8. https://doi.org/10.1038/nature25501
17. Yang Y, Chen X, Pan J et al. Pan-cancer single-cell dissection reveals phenotypically distinct B cell subtypes. *Cell* 2024; 187:4790–811.e22. https://doi.org/10.1016/j.cell.2024.06.038
18. Bankó Z, Pozsgay J, Szili D et al. Induction and differentiation of IL-10-producing regulatory B cells from healthy blood donors and rheumatoid arthritis patients. *J Immunol* 2017; 198:1512–20. https://doi.org/10.4049/jimmunol.1600218
19. Tretter T, Venigalla RK, Eckstein V et al. Induction of CD4+ T-cell anergy and apoptosis by activated human B cells. *Blood* 2008; 112:4555–64. https://doi.org/10.1182/blood-2008-02-140087
20. Huang S, Ziegler CGK, Austin J et al. Lymph nodes are innervated by a unique population of sensory neurons with immunomodulatory potential. *Cell* 2021; 184:441–59.e25. https://doi.org/10.1016/j.cell.2020.11.028
21. Mardelle U, Bretaud N, Daher C et al. From pain to tumor immunity: influence of peripheral sensory neurons in cancer. *Front Immunol* 2024; 15:1335387. https://doi.org/10.3389/fimmu.2024.1335387